Proceedings of ASME TURBO EXPO 2004
Power for Land, Sea, and Air
June 14-17, 2004, Vienna, Austria

GT2004-53258

AXIAL TURBINE TIP DESENSITIZATION BY INJECTION FROM A TIP TRENCH

PART 2: LEAKAGE FLOW SENSITIVITY TO INJECTION LOCATION

Nikhil M. Rao[1], Cengiz Camci[2]

Turbomachinery Heat Transfer Laboratory
Department of Aerospace Engineering
The Pennsylvania State University

223 Hammond Building, University Park, PA 16802

ABSTRACT

In Part 1 of this paper it was shown that discrete jets issuing from a tip platform trench were successful in reducing the total pressure deficit due to tip leakage flow. The specific tip cooling system used in Part 1 had all four injection locations active. This paper examines the effect of the individual location of the injection hole on the tip leakage flow. The investigation was carried out in a large-scale rotating rig. Total pressure downstream of the rotor exit was measured using a Kulite sensor. The measurements were phase-locked and ensemble averaged over 200 rotor revolutions. The injection holes are located at 61%, 71%, 81%, and 91% blade axial chord, in the tip trench of a single blade with a clearance of 1.40% blade height. Individual injection at 61% and 71% chord reduced the leakage vortex size. Coolant injection at 81% chord was the most successful in reducing the total pressure deficit in the leakage vortex. Injection from 91% chord had no effect on the leakage vortex. Injection from combinations of holes had greater effect in reducing the leakage vortex size and the total pressure deficit associated with the vortex. It can be concluded that the individual jets most likely turn the leakage flow towards the trailing edge. Most of the leakage flow that is responsible for the greatest total pressure deficit occurs around 80% chord.

INTRODUCTION

In Part 1 of this paper [1] it was shown that coolant injection from four injection locations, in a tip platform trench, was successful in weakening the tip leakage vortex measured downstream of a turbine rotor. The coolant flow is usually bled out from the engine HP compressor section and is essentially a penalty on the engine efficiency. Thus, as in film cooling applications, the success of this aerodynamic tip desensitization strategy depends on the optimum use of the least amount of coolant. The objective of this paper is to present investigations conducted to understand the effect each injection location has on the leakage flow. Combinations of injection locations were also studied to identify the most effective region for coolant injection.

As the leakage flow exits the tip platform a sheet of vorticity is shed into the passage. This vorticity is generated by the shear layer between the leakage flow and the tip platform. The strength of the vorticity shed depends on the leakage flow velocity. Once the vorticity enters the passage it entrains fluid from the passage resulting in the tip vortex. The size of the leakage vortex at a given measurement location depends on both the strength of the shed vorticity as well as on the chord-wise inception of the vortex itself. Bindon [2] measured total pressure in the tip gap, at gap exit, and blade passage endwall in a linear cascade and calculated the loss development along the blade chord. It was determined that at various gap sizes the total integrated endwall loss remained constant up to about 70% chord, thereafter increasing non-linearly and at a higher rate for greater clearances. Additionally, when compared to zero clearance loss, the loss with a tip gap rose rapidly after about 40% chord. The total endwall losses were broken down into three components, of which the internal gap loss and the mixing loss were found to be major contributors. Yaras et al. [3] made detailed flow measurements in the tip gap, along the blade mean line in a linear cascade. The velocity vectors close to the tip platform were found to vary rapidly in magnitude and direction, particularly closer to the trailing edge. The velocity vectors were directed towards the pressure-side in two measurement planes below 20% gap height and towards the suction-side in all planes above 25% gap height. This was attributed to the presence of a vortex due to flow separation

1 *Research Assistant, Pennsylvania State University, nmr2@psu.edu*
2 *Professor of Aerospace Engineering, Pennsylvania State University, cxc11@psu.edu*

COPYRIGHT © 2004 by ASME

over the tip platform. It was also concluded that most of the leakage flow occurred closer to the endwall. The effect of simulated rotation on tip leakage was also investigated by Yaras et al. [4, 5] in a planar cascade of turbine blades. The study concluded that relative wall motion caused a global reduction in velocity normal to camberline in the tip gap. The global velocity decreased as gap size was reduced and with increase in the relative casing motion. The flow vectors close to the wall are turned more towards the trailing edge as the relative wall velocity is increased. This is due to the no-slip condition at the wall. Additionally, the casing motion caused the separation bubble to be confined closer to the tip platform. Rotating five-hole probe measurements were conducted by McCarter et al. [6] in the large-scale rotating rig at The Pennsylvania State University. The measurements show that the leakage flow begins to develop after 70% chord. At 80% chord the leakage flow is confined to within 15% of the passage, close to the suction-side. Thereafter, the leakage flow develops rapidly, occupying 25% of the passage and 10% of the span at a passage location of 90% chord. The area mass averaged vorticity shed into the passage also more than doubled between 80% and 90% blade chord.

FACILITY DESCRIPTION

Turbine Research Facility: The facility used for the current research is the Axial Flow Turbine Research Facility (AFTRF), at The Pennsylvania State University. A detailed description of the design of this rig is available in Lakshminarayana et al. [7]. The reader is referred to Part 1 [1] for a brief description of the facility characteristics and the air transfer system that provides cooling air to rotating turbine blades.

Tip Cooled Rotor Blade: The rotor consists of 29 blades, with a design clearance of t/h=0.73% blade height. For this investigation a single test blade, with a tip clearance of 1.40% of the blade height, is used. The test blade is shown in Figure 1. The blade has a tip trench and injection holes at four locations 61%, 71%, 81%, and 91% blade axial chord. Each location is given a unique name (H1,H2,H3,H4) for easy reference, as displayed in the figure. A blade root plenum supplies the injection air to four individual radial plenums simultaneously. At 91% axial chord, the injection hole (H4) is a single radial hole (ϕ1.8 mm) that opens directly into the blade root plenum. At the other locations two holes of diameter 0.76 mm, inclined towards the blade pressure side at 45° to the radial direction are drilled. Each set opens into a single radial plenum. The blade plenum is connected via high pressure nylon tubing to the Air Transfer System (ATS). Details of the injection holes and ATS can be found in [1].

Instrumentation: A detailed description of the instrumentation is provided in [1]. For completeness a description of the total pressure probe follows. Unsteady total pressure $0.3C_{ax}$ downstream of the rotor exit is measured by a high-frequency Kulite semiconductor transducer, XCS-062-5D, and the results are ensemble averaged over 200 realizations. The Kulite dynamic pressure transducer measures the pressure differential between the rotor exit total pressure and the ambient pressure. The transducer element has a natural frequency of 150 kHz. The sensor is mounted with a screen and is known to have a flat magnitude and phase response up to 20 kHz. The transducer is flush mounted into a square cut cylindrical probe of diameter 3.5 mm. The square face gives the probe an acceptance angle of ±10°. The probe is oriented to the absolute velocity vector at the tip (25.4° CCW from axial). The probe is mounted in a stepper motor controlled radial traverse.

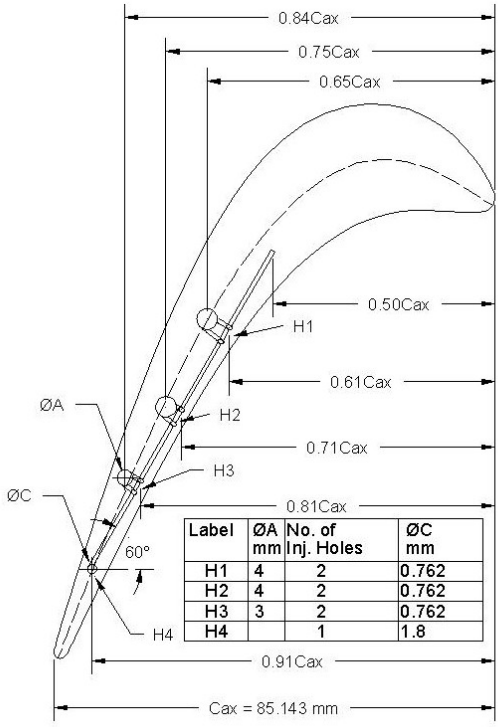

Label	ØA mm	No. of Inj. Holes	ØC mm
H1	4	2	0.762
H2	4	2	0.762
H3	3	2	0.762
H4		1	1.8

Figure 1 Geometry of Tip Injection Holes and the Tip Trench

In order to study the effect of individual holes and their combinations it was necessary to block the inactive holes. The injection holes were blocked using silicone sealant and allowed to dry for at least 24 hours. The seal was tested by pressurizing the ATS to 20 psig before each test. Care was taken to ensure that no sealant was left in the trench or sticking out onto the tip platform itself. To unblock an injection hole the ATS was again pressurized to about 15 psig and a thin wire was used to separate the silicone form the walls of the hole and allowing the pressure to blow out the plug. This procedure ensures that the geometry of the tip platform, trench, and edges of the platform with the blade surfaces are not affected.

Operation, Data Acquisition and Processing: For tests involving mass injection, the air supply was turned on 45 minutes after the turbine was started. The control valve on the air supply tank to the ATS was adjusted to achieve a plenum pressure of 10 psig and allowed to stabilize for 5 minutes, before data acquisition was commenced.

All data acquisition is controlled by virtual instruments (VI's) setup using LabView. The probe traverse mechanism and high speed data acquisition is controlled by a Pentium 4 PC with a National Instruments PCI-6110E board.

COPYRIGHT © 2004 by ASME

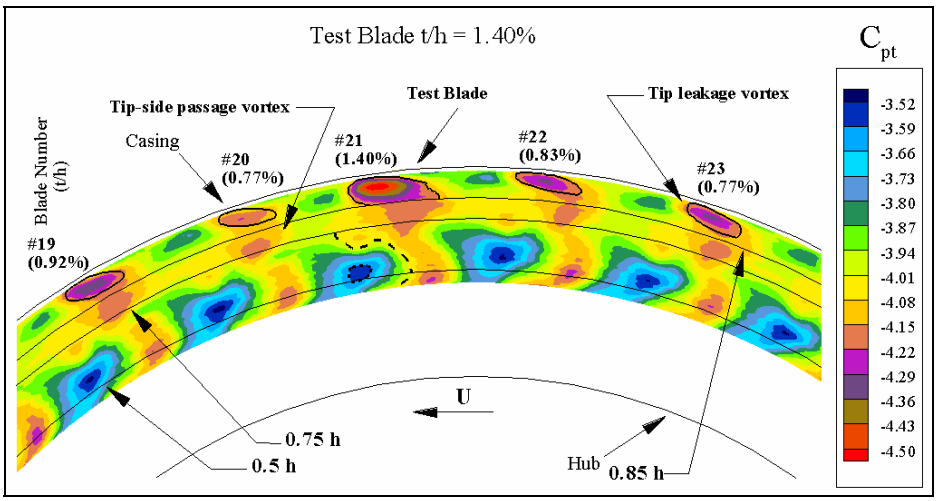

Figure 2 Base3: t/h = 1.40%, M_{inj} = 0

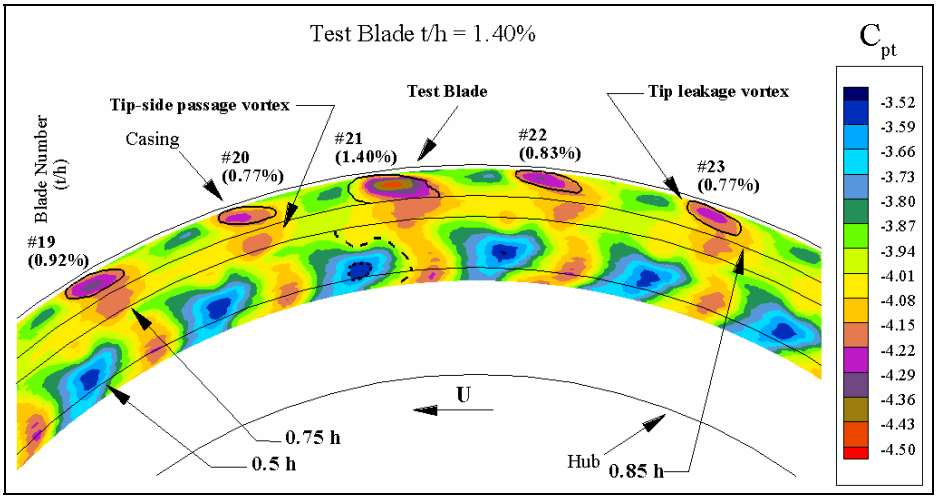

Figure 3 C_{pt} Contours: t/h = 1.40%, Injection from H1, M_{inj} = 0.2

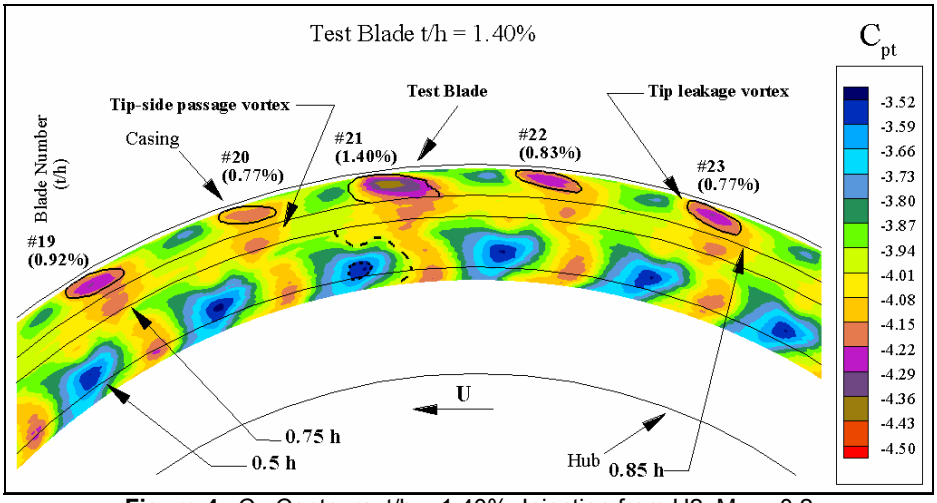

Figure 4 C_{pt} Contours: t/h = 1.40%, Injection from H2, M_{inj} = 0.2

COPYRIGHT © 2004 by ASME

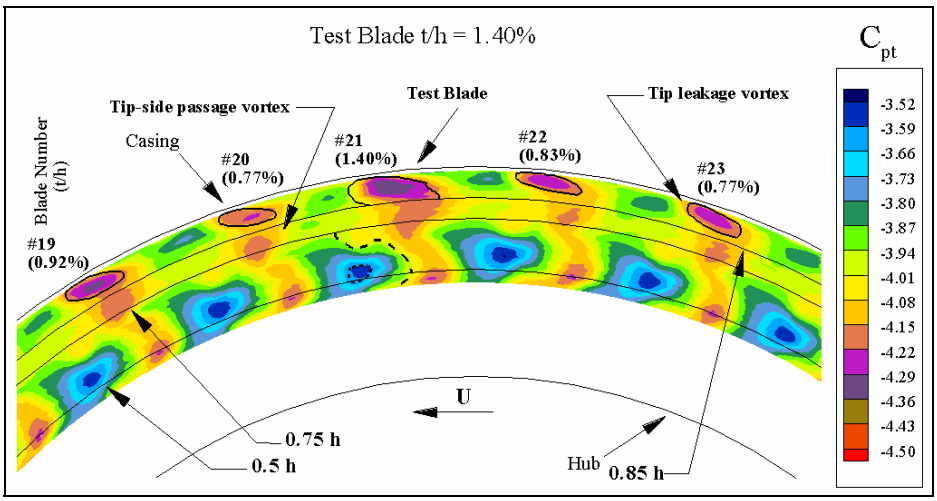

Figure 5 C_{pt} Contours: t/h = 1.40%, Injection from H3, M_{inj} = 0.2

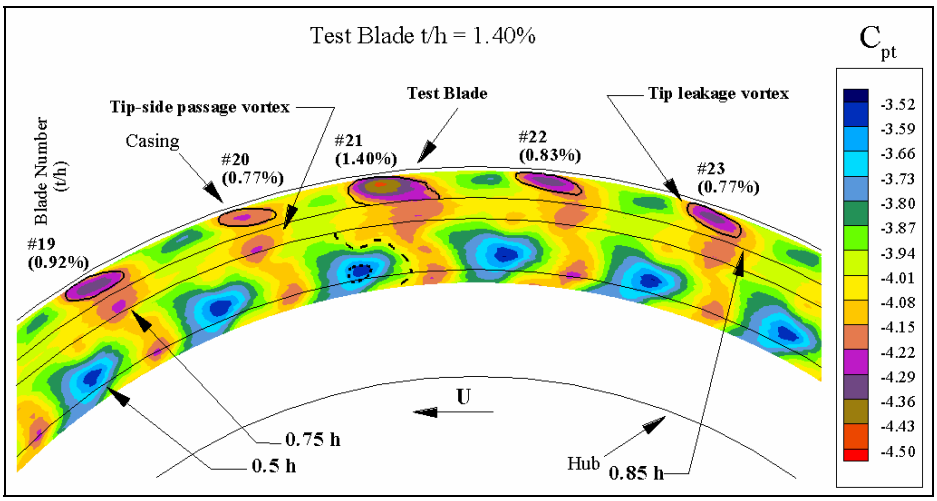

Figure 6 C_{pt} Contours: t/h = 1.40%, Injection from H4, M_{inj} = 0.3

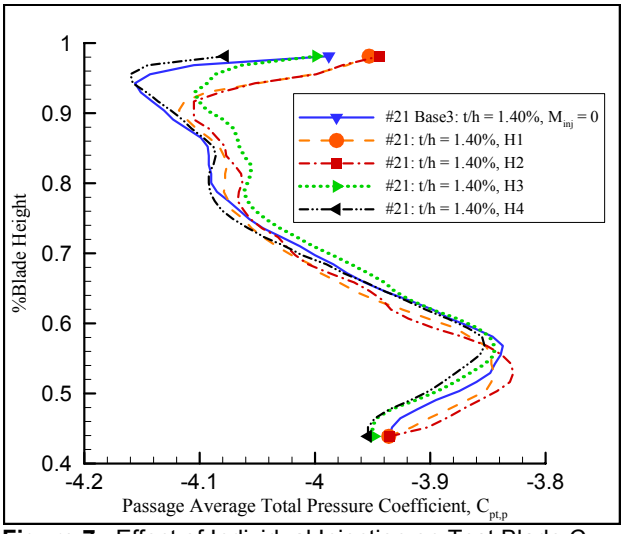

Figure 7 Effect of Individual Injection on Test Blade $C_{pt,P}$.

COPYRIGHT © 2004 by ASME

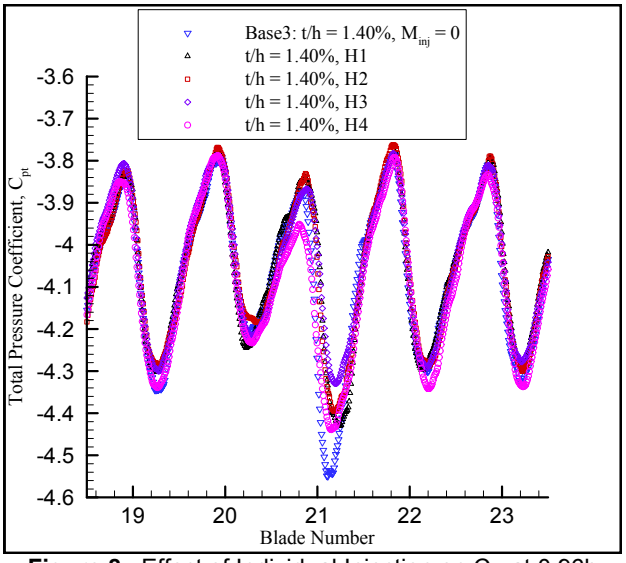

Figure 8 Effect of Individual Injection on C_{pt} at 0.96h

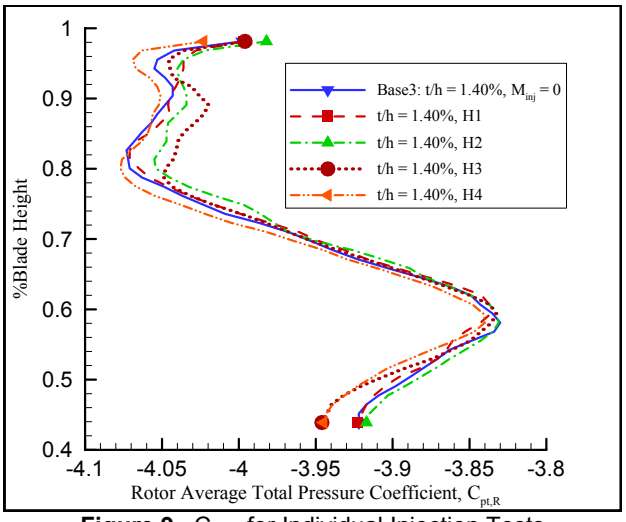

Figure 9 $C_{pt,R}$ for Individual Injection Tests

The data acquisition is initiated by a trigger pulse (1 per revolution) and is controlled by a clock pulse (6000 pulses per revolution), with both sets of digital signals being generated by an optical shaft encoder on the turbine shaft. The data acquisition is thus phase-locked at frequencies determined by the temperature corrected rotor speed. At each radial location 200 ensembles of the rotor exit absolute total pressure were acquired and averaged. The probe was moved from 0.438h to 0.981h, a total of 42 steps with a step size of 1/16 inch.

MEASUREMENT UNCERTAINTIES

The uncertainty on the measured total pressure coefficient is $\delta C_{pt} = \pm 0.024$ as explained in Part 1 of this paper [1]. The uncertainty estimation method is from Kline and McClintock [8]. The total pressure sensor used for the rotor exit flow-field measurement has a ±35 Pa absolute measurement uncertainty (± 0.1 % full scale). The dynamic pressure sensor Kulite XCS-062 did not have significant non-linearity error in the narrow range of dynamic pressure encountered in the turbine facility. The mean total pressure at the rotor exit is 94 % of the inlet total pressure that is approximately 6 kPa or 17 % full scale reading of the transducer. Other details related to uncertainty estimates are provided in [1].

EXPERIMENTAL RESULTS & DISCUSSION

The results are presented in the form of contours of ensemble averaged total pressure coefficient $C_{pt}(i,j)$, radial distributions of the passage averaged total pressure coefficient $C_{pt,P}(j)$, the rotor averaged total pressure coefficient $C_{pt,R}(j)$, and circumferential distributions of total pressure coefficient at two selected radial locations. The location 0.96h (measured from the hub) corresponds to the peak total pressure deficit in the baseline leakage vortex, while the location 0.57h corresponds to the maximum total pressure measured in the passage flow. The contour plots are the total pressure distribution at $0.3C_{ax}$ downstream of the rotor viewing upstream. Data shown is from 0.438h to 0.981h. The contour interval is 1.75% of the nominal total pressure coefficient. The radial distribution of the passage averaged and rotor averaged pressure coefficients are plotted as continuous curves, rather than points. The curve itself is generated by a three point moving average of the data with the end points unchanged. This is done to provide a better observation of the trends. The passage averaged coefficient is computed for the passage that is bounded on the suction side by the blade number referenced. So, a passage averaged coefficient for the test blade, #21, is the measured total pressure averaged across the passage that consists of the suction-side of #21 and pressure-side of # 20. The circumferential extent of the passage, over which the averaged coefficient is computed, and equations for the averaged values are as in [1]. Injection cases are referred to by the numbers of injection holes active in each case. Thus, H1 refers to injection from the location 61% chord (H1) and H1+H3 refers to combined injection from the locations 61% chord (H1) and 81% chord (H3).

Baseline Experiments: Figure 2 is a contour plot of the total pressure coefficient $0.3C_{ax}$ downstream of the rotor exit plane. The figure shows details of 5 blades, including the test blade. Radial locations corresponding to the hub, the casing, and 50%, 75%, and 85% blade span are marked. The blade number and its corresponding tip clearance, as percent of blade height, are noted above the casing boundary. The blade speed vector below the hub boundary depicts the direction of rotation. Important zones in the flow are marked out to enable easy comparison with the results of injection. The solid boundaries around the leakage vortices are drawn such that the total pressure coefficient values included in this region are -4.15 and lower. These details are reproduced in all subsequent contour plots. In all cases presented the test blade tip clearance is 1.40%.

The tip leakage vortex is clearly visible in the region above 85% span. The vortex is attached to the wake region of each blade and is characterized by low total pressure. The leakage vortex due to the enlarged tip gap of the test blade is the largest such structure observed, occupying about 15% of the blade span and extending well into the blade passage. The total pressure at the core of the test blade leakage vortex is approximately 0.2 q_m lower than that of the neighboring blades

COPYRIGHT © 2004 by ASME

shown. The total pressure gradients across this vortex are also more severe than those present in the other vortices. The vortex is not symmetric about the lowest total pressure. The low momentum flow near the suction surface of the blade is entrained more easily than the passage flow. Adjacent to the leakage vortex the passage flow exhibits a jet-like character. This flow is clearly affected by the tip leakage vortex, stretched on the pressure side and pushed in on the suction side of the structure. The maximum total pressure in this flow is also affected by the size of the leakage vortex.

Below the leakage vortex and in the blade wake lies the tip-side passage vortex, as marked in the figure. The passage vortex in the wake of the test blade exhibits the worst definition due to the stronger interaction between the two secondary flow structures. A band of lower total pressure, culminating in the tip-side passage vortex, separates the tip-side passage flow and the main passage flow structure. This might be caused by the strongly overturned flow that causes the tip-side passage vortex. The passage core occupies a large part of the passage, with the maximum total pressure near and above 50% span. In the passage containing the test blade tip leakage the maximum total pressure area is closer to 50% span than the same area in the other passages. This downward movement is probably caused by the presence of the increased leakage vortex. The passage flow moves towards the hub as it navigates the increased blockage due to the test blade leakage vortex.

Injection from individual holes: Figure 3 shows the total pressure contour for the case of injection from H1 located at 61% chord. The size of the leakage vortex has decreased as indicated by the leakage vortex and the solid boundary of the baseline leakage vortex. The leakage vortex has also moved a bit closer to the blade suction surface. The minimum total pressure measured in the leakage vortex has not changed appreciably, however the core of the vortex has shifted closer to the suction-side of the test blade. Coolant injection from H2 (at 71% chord) only, Fig. 4, also causes the test blade leakage vortex to decrease in size. The minimum total pressure measured in the vortex core is higher than that shown in Fig. 3. The reduction in leakage vortex size and the movement of the vortex core towards the suction surface may be interpreted as due to turning of the leakage flow towards the trailing edge as it passes through the tip gap. The turning is caused by the blockage due to the coolant jets. The reduction in the total pressure deficit measured in the leakage vortex may be caused by two effects. The vorticity shed into the passage is interrupted by the jets. Another reason is that the high momentum fluid from the jets is entrained by the leakage flow and this leads to higher mixing in the leakage vortex.

Figure 5 shows the effect of injecting from H3 (at 81% chord). The decrease in span-wise extent is similar to the above two cases. The minimum total pressure measured is greater by about 20% q_m. The vortex core appears to be entirely eliminated and the total pressure gradients are less severe than in the baseline. As reviewed earlier the leakage vortex was seen to increase dramatically in size between 80% and 90% chord and the area mass averaged shed vorticity also more than doubled in this region. Bindon [2] also suggests in his conceptual model that the vortex formed in the tip gap due to the separation bubble is ejected into the passage in this region. If the vortex due to the separation bubble is ejected into the passage then the total pressure deficit would not change as appreciably. Indeed, the total pressure gradients would still be present. Hence, coolant injection at 81% chord is believed to alter the leakage flow process by affecting the tip gap vortex. The coolant jet may be entrained by the vortex and the high momentum causes the vortex to diffuse substantially before it is ejected out into the passage. The jet might also have successfully blocked the separation bubble from being ejected into the passage. The passage flow above 85% blade height does appear to lose some kinetic energy. Coolant injected from H4 has very little effect on the leakage vortex, as shown in Fig. 6. The size of the vortex is about the same as that in the baseline and the low total pressure core has moved back to a location comparably similar to that found in the baseline. There is some increase in the total pressure coefficient. The more significant effect of coolant injected from H4 is the reduction in total pressure measured in the passage above 85% chord. The same effect is observed, to a lesser extent, in coolant injection from H3.

The overall effect of the isolated injection cases is more readily seen in Fig. 7, which shows the radial distribution of the passage averaged total pressure coefficient for the passage bounded by the suction-side of the test blade. Injection from H1 and H2 shows a consistent increase in the total pressure drop coefficient above 90% span. This is due to both a reduction in the area occupied by the leakage vortex as well as a marginal increase in the total pressure measured in the leakage vortex itself. Close to the casing the passage appears to be more energetic. This could be due to the entrainment of the coolant jets by the leakage flow. The slope of the total pressure drop is also remarkably steeper than in the baseline. Below 90% span the values follow that of the baseline pretty closely. Injection from H3 only is similar to the previous two cases with the exception that there is no increase in the passage average closer to the casing. In case of injection from H4 there is little change from the baseline, with the near casing total pressure actually lower by about 2%. This is caused partly by a reduction in the total pressure of the tip-side passage flow, as shown in Fig. 6.

The wake structure downstream of the blades is shown in Fig. 8. The change in wake depth follows closely what has been observed in both the contour plots and the passage average. The greatest reduction in wake depth is observed for coolant injection from H3, while the other three cases show similar reduction in depth. The similarity in the wake depth of injection cases H1, H2, and H4 is more likely due to movement of the vortex core.

The radial distribution of the rotor averaged pressure coefficient, Fig. 9, is a useful tool to determine the repeatability of various tests as it is expected that coolant injection from a single blade will not affect the flow over the entire rotor. The figure shows that the greatest variations occur between 80% and 90% span and the maximum value of this variation is approximately 0.5% of the baseline value. Additionally, the rotor averaged total pressure for coolant injection from H4 is about 1% lower than the other cases shown. This is in part responsible for the increased total pressure drop observed in the passage averaged values.

COPYRIGHT © 2004 by ASME

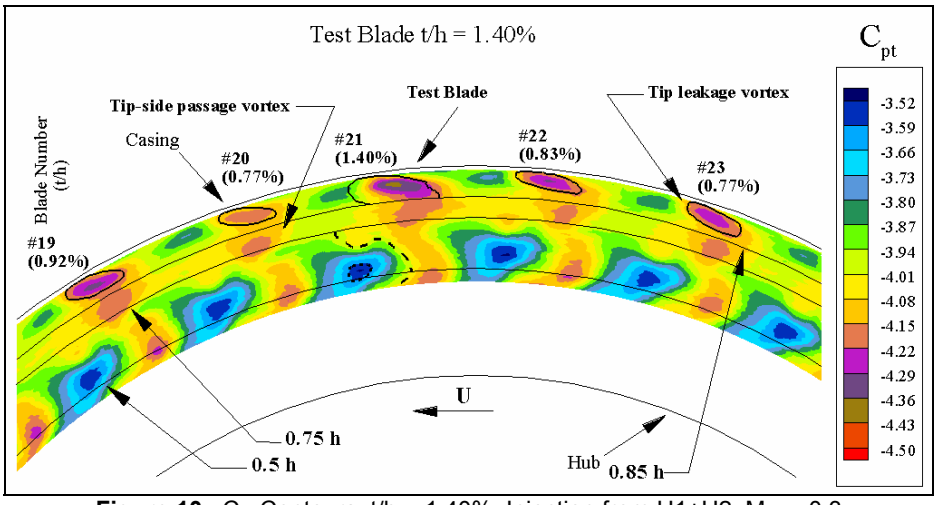

Figure 10 C_{pt} Contours: t/h = 1.40%, Injection from H1+H2, M_{inj} = 0.3

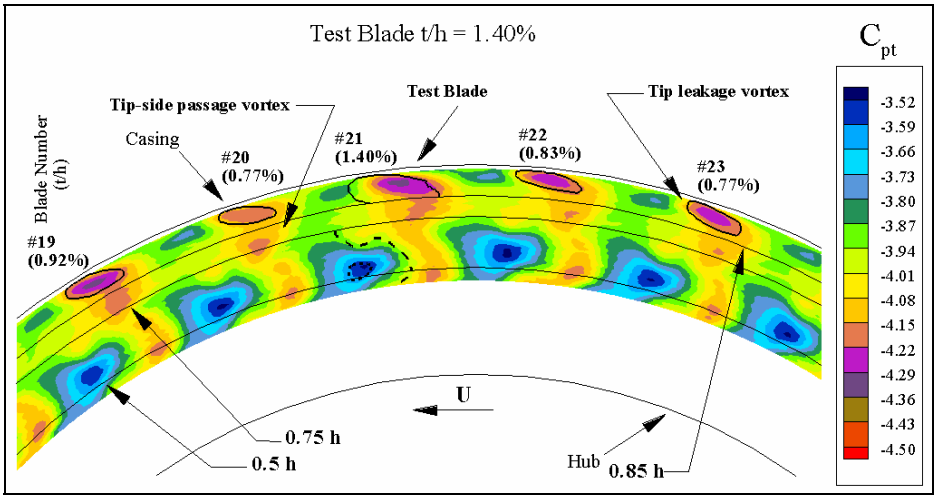

Figure 11 C_{pt} Contours: t/h = 1.40%, Injection from H1+H3, M_{inj} = 0.3

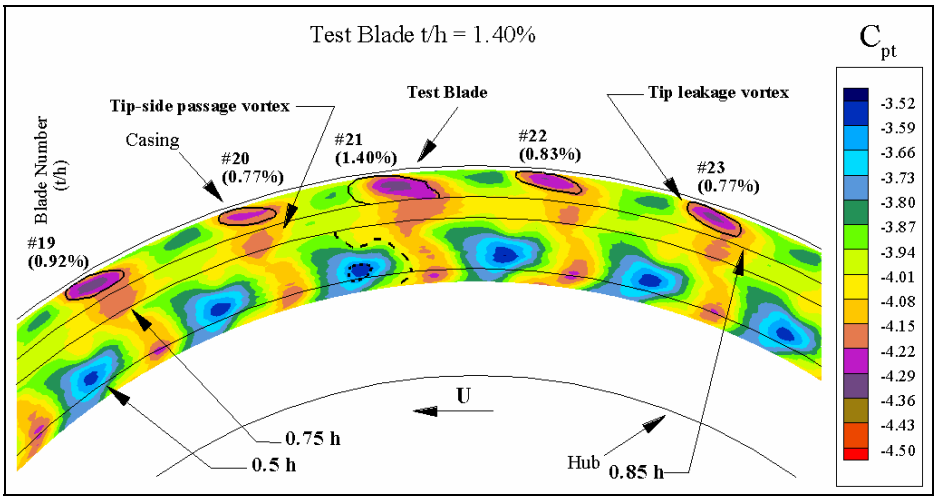

Figure 12 C_{pt} Contours: t/h = 1.40%, Injection from H2+H3, M_{inj} = 0.3

COPYRIGHT © 2004 by ASME

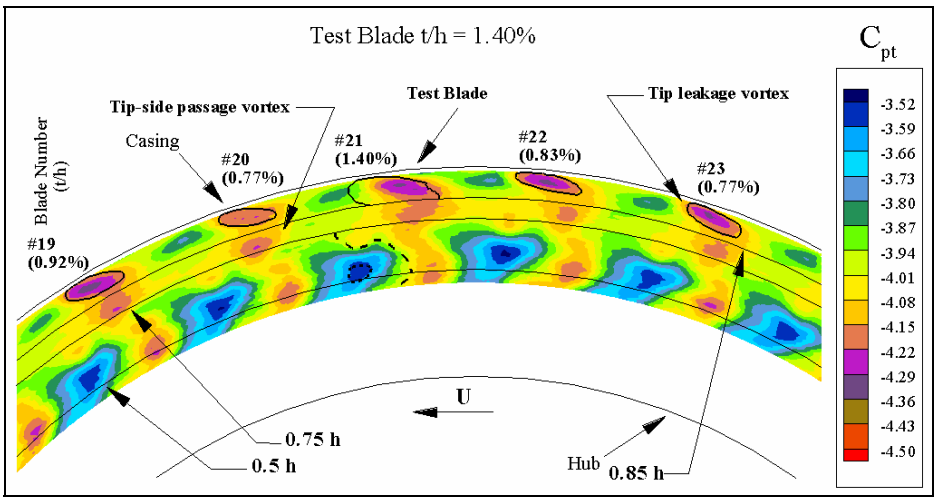

Figure 13 C_{pt} Contours: t/h = 1.40%, Injection from H1+H2+H3, M_{inj} = 0.37

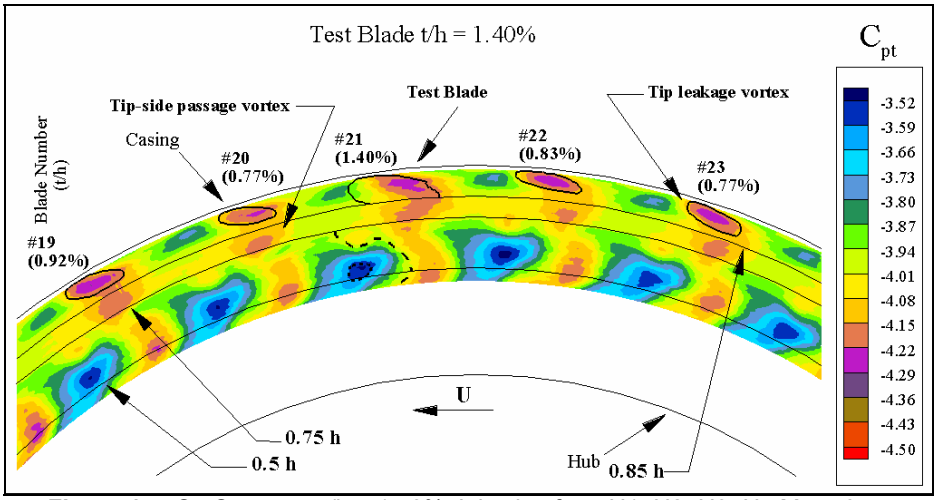

Figure 14 C_{pt} Contours: t/h = 1.40%, Injection from H1+H2+H3+H4 M_{inj} = 0.45

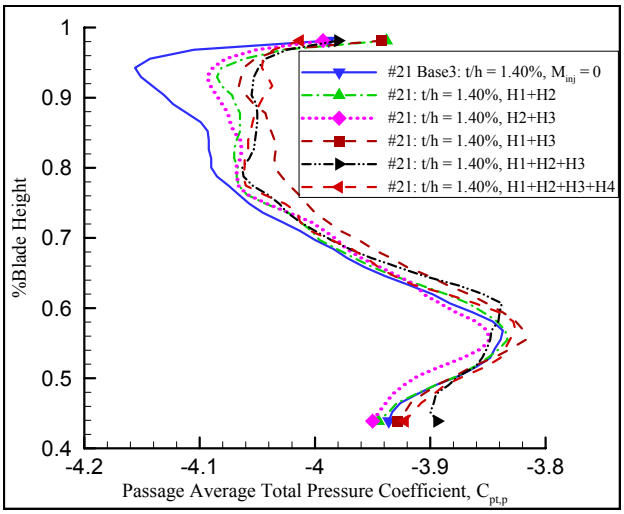

Figure 15 Effect of Combined Injection on Test Blade $C_{pt,P}$.

COPYRIGHT © 2004 by ASME

Injection from hole combinations: It is expected that injection from combination of holes will have a greater effect on the leakage flow due to the turning of the leakage flow by the individual coolant jets.

Figure 10 shows the effect of combined injection from H1 & H2. The pitch-wise extent of the tip leakage vortex is reduced more than that when individually injecting from H1 or H2. In addition, the vortex has shrunk in its span-wise extent. The decrease in measured total pressure drop, in the leakage vortex region, is also greater than the individual injection cases. Higher total pressure from the passage flow is seen within the boundary of the baseline leakage vortex, as shown by the continuous boundary of the baseline leakage vortex. When compared to the effect of individual jets from H1 & H2, the improvements in the leakage flow structure may be attributed to the turning of the leakage flow towards the trailing edge. The combination H1+H3, Fig. 11, yields similar results in terms of the area occupied by the tip leakage vortex. The total pressure deficit in the leakage vortex is reduced. The leakage vortex appears more like that of blade #19, which has a clearance of 0.92% blade height. The significance of this result is that H1 by itself is causing more of the leakage flow to develop over the last quarter of the blade chord and this allows the H3 jet to have a significant contribution in controlling the leakage flow. Coolant injection from the combination H2+H3, Fig. 12, has similar effect on the leakage vortex as the previous case, except that the pitch-wise extent of the vortex appears to have slightly increased. Based on the presentation so far it is not unexpected that when coolant is injected from H1+H2+H3 the vortex is significantly reduced and the vortex core almost vanishes, as shown in Fig. 13. There is also a reduction in the span-wise area occupied by the vortex. The effect of full blowing, H1+H2+H3+H4, is shown in Fig. 14. The total pressure distribution seen here is very similar to that of M = 0.41% presented in [1].

The passage averaged total pressure in Fig. 15 shows the extent to which the combined injection is able to recover total pressure in the passage bounded by the suction-side of the test blade. All combinations show higher averaged total pressure after coolant injection. The improvement extends to around 84% blade height, which is the zone dominated by the interaction between the passage and leakage vortices. The improvement due to all combinations shown is about the same with full blowing and the combination H1+H2+H3 showing marginally better performance. In the case of H1+H3 it is seen that below 84% blade height there appears to be significant total pressure recovery. This however is not due to injection alone, as will be discussed while presenting the rotor averaged results.

Wake plots for the injection combinations are shown in Fig. 16. In all cases it is seen that at 0.96h the wake depth is reduced. The greatest reduction occurs for the full blowing case and the least for the case H1+H2. However, there is not much difference between the cases. The most interesting feature, in comparing Fig. 8 and Fig. 16, is that the test blade wake profile is observably shifted towards the blade suction-side. This behavior is not observed for the individual injection cases. This means that combined injection is successful in moving the tip leakage vortex closer to the blade suction-side.

Figure 17 shows the rotor averaged total pressure coefficient for the various combinations. In general there is good repeatability, except in the case of H1+H3, where the curve below 88% blade height is shifted to the right. This means that for the particular test the rotor flow was slightly different from the baseline. The same behavior was observed in the passage averaged results for this case and hence it is not possible to separate the effect of coolant injection, if any, on the flow in this region.

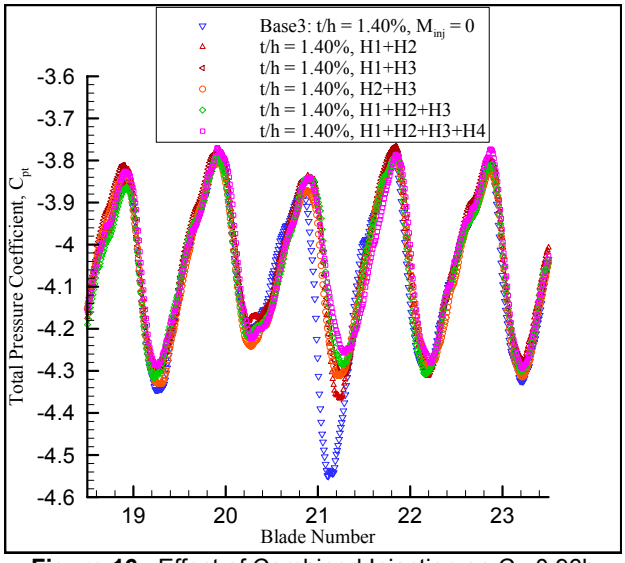

Figure 16 Effect of Combined Injection on C_{pt} 0.96h

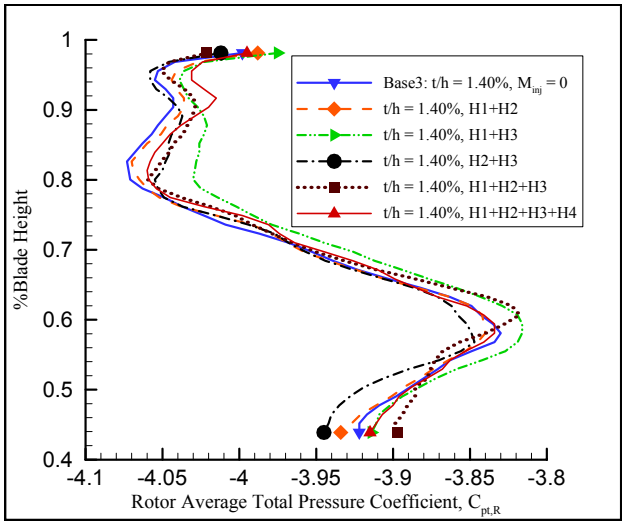

Figure 17 $C_{pt,R}$ for Combined Injection Tests

CONCLUSIONS

Turbine tip desensitization by tip coolant injection from a tip trench was investigated. In this part the focus was on investigating the effect of individual injection location and seeking an optimum combination of injection to minimize the leakage flow.

Individual injection results show that coolant injection from 61%, 71%, and 81% chord locations reduce the leakage vortex size at the measurement location. This is attributed to a

COPYRIGHT © 2004 by ASME

reduction in shed vorticity, as well as a turning of the leakage flow towards the trailing edge.

Injection from 81% chord is the most successful in filling the total pressure defect in the vortex core. Thus it appears that leakage flow responsible for the greatest total pressure deficit occurs around 80%.

The injection location at 91%, with the largest hole diameter of 1.8 mm, does not have a significant effect on the leakage flow. This hole is very close to the trailing edge of the blade. However, the tip-side passage flow shows an increase in the total pressure drop coefficient.

Combined injection in general shows better desensitization. There is observable movement of the leakage vortex towards the suction-side of the test blade. Combined injection from H1-H3 is found to be almost as effective as injection from all locations.

ACKNOWLEDGMENTS:

The research effort was initiated during our early discussions with Drs. B. Glezer and R. Bunker. The authors are thankful to Drs. L. Golan and R. Wenglarz of SCIES/HEET for their initial support. The mechanical design, manufacturing and assembly of the tip cooling system were possible because of the continuous involvement of Dr. D. Dey, G. Sayers, and H. Houtz in Penn State. The authors are also indebted to late Prof. Lakshminarayana for his constructive criticism and suggestions over the years the AFTRF was developed into a fully operational turbine research facility.

NOMENCLATURE

C_{ax}	Rotor tip axial chord length = 0.08514m
C_{pt}	Pressure coefficient $C_{pt}(i,j) = \dfrac{\overline{P}_{03}(i,j) - P_{01}}{0.5\rho U_m^2}$
$C_{pt,P}$	Passage averaged coefficient $C_{pt,P}(j) = \sum_{i}^{i+206} C_{pt}(i,j)$
$C_{pt,R}$	Rotor average coefficient $C_{pt,R}(j) = \sum_{i=1}^{6000} C_{pt}(i,j)$
M_{inj}	Coolant to free stream mass flow rate ratio
U_m	Mean wheel speed at rotor mid-span, m/sec
h	Rotor blade height = 0.123 m
i	Circumferential index
j	Radial index
p_{o1}, P_{o1}	Stage inlet total pressure, Pa
p_{o3}, P_{o3}	Stage exit total pressure, Pa
r/h	Non-dimensional radial position measured from hub
q_m	Mean kinetic energy based on U_m, Pa
t	Gap height between blade tip and outer casing, m
α_3	Rotor exit abs. velocity vector angle at tip, degrees
ϕ	Diameter of injection hole, mm
ρ	Density, kg/m^3
#	Blade number

REFERENCES

1. Rao, N. M., Camci, C., 2004, "Axial Turbine Tip Desensitization by Injection from a Tip Platform Trench. Part 1- Effect of Injection Mass Flow Rate," ASME Paper No. GT2004-53256.
2. Bindon, J. P., 1989, "The Measurement and Formation of Tip Clearance Loss," ASME J. of Turbomachinery, **111**, pp. 257-263, Paper No. 88-GT-203.
3. Yaras, M., Zhu, Y., Sjolander, S. A., 1989, "Flow Field in the Tip Gap of a Planar Cascade of Turbine Blades," ASME J. of Turbomachinery, **111**, pp. 276-283., Paper No. 88-GT-29.
4. Yaras, M. I., Sjolander, S. A., 1992, "Effects of Simulated Rotation on Tip Leakage in a Planar Cascade of Turbine Blades. Part 1: Tip Gap Flow," ASME J. of Turbomachinery, **114**, pp. 652-659, Paper No. 91-GT-127.
5. Yaras, M. I., Sjolander, S. A., Kind, R. J., 1992, "Effects of Simulated Rotation on Tip Leakage in a Planar Cascade of Turbine Blades. Part 2: Downstream Flow Field and Blade Loading," ASME J. of Turbomachinery, **114**, pp. 660-667, Paper No. 91-GT-128.
6. McCarter, A., Xiao, X., Lakshminarayana, B., 2000, "Tip Clearance Effects in a Turbine Rotor: Part 2- Velocity Field and Flow Physics," ASME Paper No. 2000-GT-477.
7. Lakshminarayana, B., Camci, C., Halliwell, I., Zaccaria, M., 1996, "Design and Development of a Turbine Research Facility to Study Rotor-Stator Interaction Effects," International Journal of Turbo and Jet Engines, **13**, pp.155-172.
8. Kline, S. J., McClintock, F. A., 1953, "Describing Uncertainties in Single-Sample Experiments," Mechanical Engineering, **75**, pp.3-8.

COPYRIGHT © 2004 by ASME